

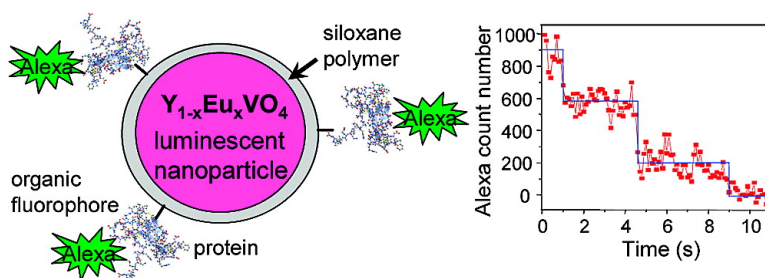
Communication

## Counting the Number of Proteins Coupled to Single Nanoparticles

Didier Casanova, Domitille Giaume, Mlanie Moreau, Jean-Louis Martin, Thierry Gacoin, Jean-Pierre Boilot, and Antigoni Alexandrou

*J. Am. Chem. Soc.*, **2007**, 129 (42), 12592-12593 • DOI: 10.1021/ja0731975 • Publication Date (Web): 29 September 2007

Downloaded from <http://pubs.acs.org> on February 14, 2009



### More About This Article

Additional resources and features associated with this article are available within the HTML version:

- Supporting Information
- Links to the 3 articles that cite this article, as of the time of this article download
- Access to high resolution figures
- Links to articles and content related to this article
- Copyright permission to reproduce figures and/or text from this article

[View the Full Text HTML](#)

## Counting the Number of Proteins Coupled to Single Nanoparticles

Didier Casanova,<sup>†</sup> Domitille Giaume,<sup>‡</sup> Mélanie Moreau,<sup>‡</sup> Jean-Louis Martin,<sup>†</sup> Thierry Gacoin,<sup>‡</sup>  
Jean-Pierre Boilot,<sup>‡</sup> and Antigoni Alexandrou<sup>\*†</sup>

Laboratoire d'Optique et Biosciences and Laboratoire de Physique de la Matière Condensée, Ecole Polytechnique,  
CNRS, 91128 Palaiseau, France, and INSERM U696, 91128 Palaiseau, France

Received May 6, 2007; E-mail: antigoni.alexandrou@polytechnique.fr

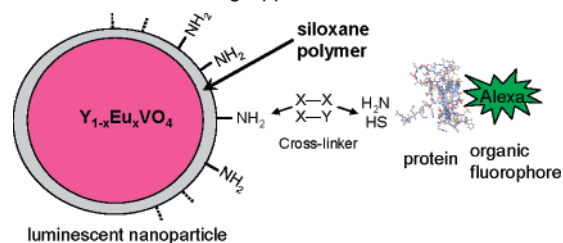
Obtaining specific coupling and quantifying the biomolecule–fluorophore ratio are important issues when coupling fluorophores to biomolecules for observation in biological assays and cells. In the case of genetic constructs employing fluorescent protein labels, the protein-label stoichiometry is intrinsically 1:1. Fluorescent proteins, however, present the disadvantage of fast photobleaching. In the past decade, luminescent nanoparticles (NPs), such as quantum dots (QDs) and lanthanide-ion-doped oxide NPs have therefore been used because of their extreme photostability compared to organic labels.<sup>1–9</sup> Given the NP size, a large number of proteins or other biomolecules can be attached to them. Ensemble measurements have been used to quantify the protein-NP coupling ratio but give no information on its distribution. Gel electrophoresis was employed to separate QD-Au<sup>10</sup> and NP-PEG conjugates<sup>11</sup> and to determine the presence of protein-QD ratios of 0:1, 1:1, 2:1, and 3:1.<sup>12</sup> The information obtained, however, remains qualitative and often suffers from the overlap between the mobility shift bands of different species. Especially in the case of proteins small compared to the NP size and of NP surface charge and size heterogeneity, electrophoretic methods can turn out complex or even inapplicable.

In this Communication, we propose a double labeling approach to determine the protein-NP stoichiometry *at the single particle level*. We coupled lanthanide-ion doped oxide NPs to a protein,  $\alpha$ -bungarotoxin, already labeled with an organic fluorophore (Alexa488, Molecular Probes) with a 1:1 stoichiometry. We then used the stepwise photobleaching of the organic fluorophores attached to individual NPs to quantify the protein-NP ratio for each NP as well as its distribution.

Single-molecule photobleaching of organic fluorophores has been exploited in the past for a variety of applications like ascertaining the presence of Ca<sup>2+</sup>-channel aggregates,<sup>13</sup> counting the number of ion channel units,<sup>14</sup> and precise localization of multiple close-lying fluorophores.<sup>15–17</sup> We here demonstrate that it allows quantification of the number of proteins per NP.

We implemented a functionalization scheme for 20 ± 4 nm (see Figure S1 for the nanoparticle size distribution) Y<sub>0.6</sub>Eu<sub>0.4</sub>VO<sub>4</sub> NPs involving a silica coating followed by an amino-organosilane layer similar to that used for QDs.<sup>18</sup> We then used a homo- or hetero-bifunctional cross-linker with two succinimidyl ester groups or one succinimidyl ester and one maleimide group that can bind in a first step to the nanoparticle amine groups and in a second one to the protein amine or sulfhydryl groups (see Scheme 1 and Supporting Information). By varying the protein concentration during the second coupling step, we obtained average protein-NP coupling ratios of 8 ± 0.8, 0.85 ± 0.04, and 0.3 ± 0.01, determined from ensemble measurements. Results on the sample with an average protein-NP ratio of 8 are shown in the following.

**Scheme 1.** Double-Labeling Approach



We spincoated NP- $\alpha$ -bungarotoxin-Alexa488 conjugates on a silica coverslip at low concentration allowing single particle observation and measured alternatively the NP (Figure 1A) and the Alexa488 emission (Figure 1B) in pH = 7.4 phosphate buffer. We observe 90% of matching between the bright spots in the NP and in the Alexa image indicating efficient NP-protein coupling. Some NPs (4%) are not coupled with proteins as expected for a Poisson distribution, whereas the presence of Alexa emission spots in the absence of a corresponding NP emission can be attributed to NP sizes too small to be detected (<13 nm).<sup>19</sup>

We then analyzed the fluorescence evolution of Alexa bright spots corresponding to protein-Alexa molecules attached to single NPs (Figure 2): we clearly observe stepwise photobleaching indicating the presence of a low discrete number of fluorophores. By simply counting the number of bleaching steps we precisely measure the number of proteins per NP. Furthermore, a histogram of the initial Alexa count number shows multiple peaks (Figure 3). The initial values of 140 and 900 counts in Figure 2 correspond to the first and third peak of the histogram (one and three proteins per NP) and are in agreement with our observation of one and three steps, respectively. Moreover, the mean initial count number for all Alexa spots presenting one, two, three, and four bleaching steps is 191 ± 109, 449 ± 151, 665 ± 260, and 1107 ± 207, respectively, in agreement with the peaks observed in the histogram of Figure 3 for which a multiple Gaussian fit gives 176 ± 176, 486 ± 29, 763 ± 94, and 1266 ± 87, respectively. The top left circle graph in Figure 3 shows the distribution of Alexa molecules per NP as determined from the surface under the Gaussians used to fit the histogram.

The mean initial count number for 379 Alexa emission spots in the single-particle measurements gives a ratio of 7.9 ± 0.5, in agreement with the ensemble result. The maximum of the coupling ratio distribution lies, however, at 3 proteins/NP (see Figure 3). Indeed, the presence of large NPs coupled to a large number of proteins (Figure S2) leads to an average ratio determined from ensemble measurements that is higher than the maximum of the coupling ratio distribution. (Similarly, in the case of organic acceptor molecules attached to QD donors, Pons et al.<sup>20</sup> demonstrated that the single-particle fluorescence resonance energy transfer efficiency may deviate from that obtained from ensemble measurements.) Our

<sup>†</sup> Laboratoire d'Optique et Biosciences and INSERM U696.

<sup>‡</sup> Laboratoire de Physique de la Matière Condensée.

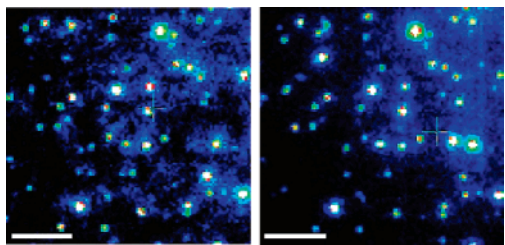


**Figure 1.** Wide-field fluorescence microscopy images of individual NP- $\alpha$ -bungarotoxin-Alexa488 conjugates spincoated on a coverslip: (left) image of the NP emission at 617 nm (integration time, 500 ms; laser intensity, 2–3 kW/cm<sup>2</sup>); (right) image of the Alexa488 emission centered at 519 nm (integration time, 30 ms; laser intensity, 0.7–1 kW/cm<sup>2</sup>). Scale bar = 5  $\mu$ m.

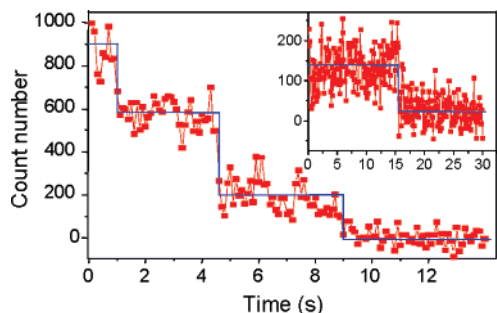


**Figure 2.** Time evolution of a single Alexa emission spot showing three (main figure) and one (inset) photobleaching steps. Blue lines help visualize the steps. Integration time, 100 ms; laser intensity, 0.07–0.1 kW/cm<sup>2</sup>.

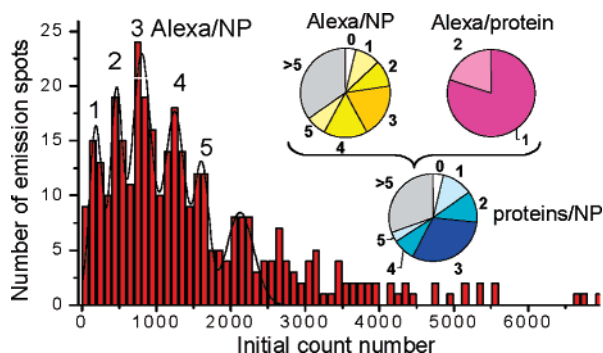


**Figure 3.** Histogram of the initial count number for 379 individual Alexa emission spots. The solid line is the fit of the histogram for count numbers 0–2400 using 6 Gaussians. Experimental conditions as in Figure 2. The large count number part of the histogram is not shown. Circle graphs show the distribution of Alexa molecules per NP, Alexa molecules per protein, and proteins per NP. The percentages corresponding to each sector are given in Tables S1 and S2.

single-particle technique, on the other hand, measures the complete protein-NP coupling ratio distribution.

Obviously, a necessary requirement for the application of this method is to obtain proteins labeled with one organic fluorophore. This is easily achievable with electrophoretic methods for proteins which have a precise molecular weight and was commercially available for the protein used here. In addition, exactly the same photobleaching step counting technique can be used to determine the number of fluorophores per protein. In our case, 80% of the proteins were labeled with one Alexa and 20% with two (see circle graph in Figure 3). Using this information, the distribution of proteins per NP could be precisely calculated (see bottom circle graph in Figure 3).

In conclusion, we coupled lanthanide-ion doped oxide NPs to proteins and measured the protein-NP coupling ratio at the single-particle level and its distribution based on the stepwise photobleaching and the initial emission of organic fluorophores labeling the protein molecules. Our single-particle, double-tag imaging technique further allows selecting in situ NPs coupled to the desired number of proteins, a feature essential for cell imaging and biological assay experiments. Indeed, we can envisage measuring the photobleaching steps of the organic fluorophore and then selectively analyzing trajectories or other features of only those nanoparticles coupled, for instance, to a single protein or to two proteins and even compare the results for different protein-NP coupling ratios. This approach is applicable to all types of NP labels, such as semiconductor or metallic NPs, and biomolecules.

**Acknowledgment.** We are grateful to B. Dubertret and M. Négrerie for fruitful discussions. We thank the DGA (Délégation Générale pour l'Armement) and the Fonds National pour la Science (AC Dynamique et Réactivité des Assemblages Biologiques) for financial support.

**Supporting Information Available:** Experimental procedures, Figures S1 and S2, Tables S1 and S2. This material is available free of charge via the Internet at <http://pubs.acs.org>.

## References

- (1) Michalet, X.; Pinaud, F. F.; Bentolila, L. A.; Tsay, J. M.; Doose, S.; Li, J. J.; Sundaresan, G.; Wu, A. M.; Gambhir, S. S.; Weiss, S. *Science* **2005**, *307*, 538–544.
- (2) Medintz, I. L.; Uyeda, H. T.; Goldman, E. R.; Mattoussi, H. *Nat. Mater.* **2005**, *4*, 435–446.
- (3) Beaurepaire, E.; Buisette, V.; Sauviat, M.-P.; Giaume, D.; Lahlil, K.; Mercuri, A.; Casanova, D.; Huignard, A.; Martin, J.-L.; Gacoin, T.; Boilot, J.-P.; Alexandrou, A. *Nano Lett.* **2004**, *4*, 2079–2083.
- (4) Meiser, F.; Cortez, C.; Caruso, F. *Angew. Chem., Int. Ed.* **2004**, *43*, 5954–5957.
- (5) Yi, G.; Lu, H.; Zhao, S.; Ge, Y.; Yang, W.; Chen, D.; Guo, L.-H. *Nano Lett.* **2004**, *4*, 2191–2196.
- (6) Lu, H.; Yi, G.; Zhao, S.; Chen, D.; Guo, L.-H.; Cheng, J. *J. Mater. Chem.* **2004**, *14*, 1336–1341.
- (7) Louis, C.; Bazzi, R.; Marquette, C. A.; Bridot, J.-L.; Roux, S.; Ledoux, G.; Mercier, B.; Blum, L.; Perriat, P.; Tillement, O. *Chem. Mater.* **2005**, *17*, 1673–1682.
- (8) Dosev, D.; Nichkova, M.; Liu, M.; Guo, B.; Liu, G.-Y.; Hammock, B. D.; Kennedy, I. M. *J. Biomed. Opt.* **2005**, *10*, 064006.
- (9) Diamante, P. R.; Burke, R. D.; van Veggel, F. C. *Langmuir* **2006**, *22*, 1782–1788.
- (10) Fu, A.; Micheel, C. M.; Cha, J.; Chang, H.; Yang, H.; Alivisatos, A. P. *J. Am. Chem. Soc.* **2004**, *126*, 10832–10833.
- (11) Sperling, R. A.; Pellegrino, T.; Li, J. K.; Chang, W. H.; Parak, W. J. *Adv. Funct. Mater.* **2006**, *16*, 943–948.
- (12) Pons, T.; Uyeda, H. T.; Medintz, I. L.; Mattoussi, H. *J. Phys. Chem. B* **2006**, *110*, 20308–20316.
- (13) Harms, G. S.; Cagnet, L.; Lommerse, P. M. H.; Blab, G. A.; Kahr, H.; Gamsjäger, R.; Spaink, H. P.; Soldatov, N. M.; Romanin, C.; Schmidt, T. *Biophys. J.* **2001**, *81*, 2639–2646.
- (14) Ulbrich, M. H.; Isacoff, E. Y. *Nat. Meth.* **2007**, *4*, 319–321.
- (15) Gordon, M. P.; Ha, T.; Selvin, P. R. *Proc. Natl. Acad. Sci. U.S.A.* **2004**, *101*, 6462–6465.
- (16) Qu, X.; Wu, D.; Mets, L.; Scherer, N. F. *Proc. Natl. Acad. Sci. U.S.A.* **2004**, *101*, 11298–11303.
- (17) Betzig, E.; Patterson, G. H.; Sougrat, R.; Lindwasser, O. W.; Olenych, S.; Bonifacino, J. S.; Davidson, M. W.; Lippincott-Schwartz, J.; Hess, H. F. *Science* **2006**, *313*, 1642–1645.
- (18) Gerion, D.; Pinaud, F.; Williams, S. C.; Parak, W. J.; Zanchet, D.; Weiss, S.; Alivisatos, A. P. *J. Phys. Chem. B* **2001**, *105*, 8861–8871.
- (19) Casanova, D.; Giaume, D.; Beaurepaire, E.; Gacoin, T.; Boilot, J.-P.; Alexandrou, A. *Appl. Phys. Lett.* **2006**, *89*, 253103.
- (20) Pons, T.; Medintz, I. L.; Wang, X.; English, D. S.; Mattoussi, H. *J. Am. Chem. Soc.* **2006**, *128*, 15324–31.

JA0731975